Nuclear Transport in 3T3 Fibroblasts: Effects of Growth Factors, Transformation, and Cell Shape

Lian-Wei Jiang and Melvin Schindler

Department of Biochemistry, Michigan State University, East Lansing, Michigan 48824

Abstract. Nucleocytoplasmic transport of fluorescent-labeled macromolecules was investigated in transformed and nontransformed 3T3 fibroblasts. Insulin and epidermal growth factor enhanced transport threefold after 1–2-h incubation with nontransformed adhering fibroblasts; no enhancement of transport was observed for spherical unattached fibroblasts. The concentration of growth factor for maximal enhancement was 3–10 nM. Nuclear transport for Kirsten murine sarcoma virus–transformed BALB/c 3T3 fibroblasts, however, was maximally enhanced before addition of growth factors; addition of insulin or epidermal growth factor causes no additional transport enhancement. Transformation also minimizes cell shape effects on macromolecular nuclear transport. These results provide evidence that protein growth factors and oncogenic transformation may use a similar mechanism for activation of nuclear transport.

PROTEIN growth factors serve as cell-specific mediators of cellular communication (11). Through interactions with cell surface receptor proteins, protein growth factors specific for individual cell types can trigger a repertoire of transcriptional or replicational responses. Although much work has detailed the initial event (protein growth factor/receptor binding) in the signaling pathway, the means by which subsequent mRNA production and transport is activated remains fertile ground for speculation. Inasmuch as protein growth factors are internalized with their receptors and transported into the cytoplasmic compartment, a number of groups have explored the possibility that these growth factors may be delivered to the nucleus either in free form or in association with their respective receptors (7, 13, 22, 31, 32). Results of binding studies with insulin (6, 7, 34), epidermal growth factor (EGF)[1] (13), and nerve growth factor (17, 31, 36, 37) to isolated nuclei and whole cells give evidence for protein growth factor receptor localization at the inner nuclear membrane/lamina surface. Functionally, in the case of nerve growth factor, nuclear binding appears to be essential for the differentiating signals that initiate neurite outgrowth (31). With regard to insulin, enhanced mRNA (21, 30) and macromolecular transport (12, 25) have been observed after insulin addition to isolated nuclei. Recent work from our laboratory has attempted to directly measure the effect of insulin and EGF on the bidirectional transport of macromolecules through the nuclear pore complex (25). These measurements demonstrated that insulin and EGF could significantly enhance macromolecular transport in isolated nuclei within the concentration range used for assessing the binding of insulin and EGF to nuclear and plasma membrane receptors. Here we extend these studies to in vivo systems. Enhancement (about threefold) of nucleocytoplasmic transport is observed in 3T3-1 and BALB/c 3T3 fibroblasts stimulated by the addition of insulin or EGF. Such an EGF-induced transport rate enhancement is not observed for 3T3-NR6 fibroblasts, a mutant cell line not expressing the EGF receptor (20, 29). Shape appears to have a role in these protein growth factor responses, since cells maintained in a spherical state during measurements do not demonstrate enhanced nuclear transport as a function of protein growth factor addition. Of particular interest is the result that nuclear transport in Kirsten murine sarcoma virus–transformed (3T3-KMuSV) BALB/c 3T3 fibroblasts is already maximally stimulated in the absence of insulin and EGF. Subsequent addition of these growth factors has little effect.

The data presented here may be interpreted to suggest that: (*a*) protein growth factors enhance the bidirectional, diffusion-mediated nuclear transport of macromolecules in 3T3 fibroblasts; (*b*) transport is correlated with receptor–ligand affinity; (*c*) response in untransformed cells is related to cell shape; and (*d*) transformed fibroblasts have maximally stimulated nuclear transport rates and are refractory towards exogenously supplied insulin and EGF. The latter result would suggest that the mechanisms of protein growth factor and oncogenic stimulation that have similarities at the transmitter side of the cellular signaling pathway (plasma membrane–receptor level) may also share common activation features at the putative receiver (nuclear surface).

Materials and Methods

Reagents

Fluorescein-labeled dextrans (20,000 and 70,000 mol wt, designated 20K and 70K, respectively) and thymidine were obtained from Sigma Chemical Co. (St. Louis, MO). Tritiated thymidine (10 Ci/mmol) was from ICN Radio-

1. *Abbreviations used in this paper*: EGF, epidermal growth factor; KMuSV, Kirsten murine sarcoma virus.

chemicals (Irvine, CA). Porcine insulin, EGF, and glucagon were from Gibco (Grand Island, NY); Collaborative Research, Inc. (Lexington, MA), and Sigma Chemical Co., respectively. Plasma fibronectin (bovine) was purchased from Calbiochem-Behring Corp. (La Jolla, CA). Bovine insulin chain A was from Sigma Chemical Co. Untransformed BALB/c A31 and Kirsten murine sarcoma virus-transformed 3T3 BALB/c A31 and 3T3-1 (3T3-Swiss albino) cell lines were obtained from American Type Culture Collection (Rockville, MD). The 3T3-NR6 EGF nonresponsive cell line isolated from murine Swiss albino 3T3 cells was a kind gift of Dr. H. R. Herschman, Laboratory of Biomedical and Environmental Sciences, University of California, School of Medicine (Los Angeles, CA).

Cell Growth and Synchrony

The double thymidine block was applied to induce synchrony at the G_1/S interphase for BALB/c 3T3, 3T3-1 (Swiss 3T3), and Kirsten murine sarcoma virus (KMuSV)-transformed BALB/3T3. 1.2×10^6 cells were plated on 75 cm^2 tissue/culture flask and grown in DME supplemented with 10% calf serum and 3 mM thymidine. After 18 h, the medium was changed to a fresh medium lacking thymidine. After another 6-h incubation and washing, 3 mM thymidine was added again for a 24-h culture, followed by washing two times with DME. 80–90% of the cells then were released into G_1/S interphase synchronously (1) as indicated in DNA synthesis assay and were then ready for fluorescein dextran scrape-loading.

Fluorescent Dextran Incorporation into Fibroblasts and Cellular Fluorescence Analysis

The synchronized cells were subjected to the scrape-loading procedure (18), as modified by us (26), using 10 mg/ml of 20K or 70K fluorescein dextrans in DME. G_1/S phase cells, after scrape-loading, were suspended in DME and replated in 35-mm tissue culture dishes for ~3 h. Both spherical and spread cell samples were then ready for nuclear fluorescence photobleaching (12, 16, 25, 26) or fluorescence intensity (ACAS 470 Interactive Laser Cytometer; Meridian Instruments, Inc., Okemos, MI) (28, 35) within 1–3 h.

Nuclear Fluorescence Photobleaching of Fibroblasts and Cell Fluorescence Analysis

Lang et al. (16) point out that an important consideration in performing nuclear photobleaching in vivo is that tissue culture cells usually display a large nucleoplasmic/cytoplasmic volume ratio. The subsequent bleaching of the nucleus renders most of the cellular fluorescent pool nonfluorescent and results in a recovery to an equilibrium value that is much lower than the prebleach fluorescence intensity. The problem in the interpretation of this data, as clearly formulated by Lang et al. (16), is that the influx rate constant K, which under conditions of an infinitely large cytoplasmic pool of fluorescent probe, is independent of the cytoplasmic volume:

$$K = (S_N/V_N)P,$$

where S_N and V_N are the surface area and volume of the nucleus, respectively. Under conditions of comparable nuclear and cytoplasmic volume, however, K is represented as:

$$K = [S_N(1/V_N + 1/V_C)]P,$$

where V_C is the cytoplasmic volume. Incomplete recoveries under the latter scenario could either represent a volume effect or an immobile fraction. We attempted to overcome this problem of interpretation by using two technical approaches. To insure a metabolically homogeneous population of cells for analysis and to minimize cell-to-cell volume and extent of attachment variation, we chose to synchronize our cell cultures. Careful selection of single living cells was performed to insure a large V_C/V_N ratio. In addition, we enhanced our fluorescent probe signal by scrape-loading rather than microinjecting. Concentrations of 0.3–0.5 mM fluorescent dextrans could be reached as opposed to ~10 μM for microinjection. Since we had sufficient signal to monitor recovery, repeated bleaching could be performed on the same cell to properly interpret incomplete fluorescence recovery. Fluorescence bleaching experiments were performed as discussed previously (12) for isolated nuclei and (26) for whole cells. Interactive laser cytometric imaging was performed as described previously (28).

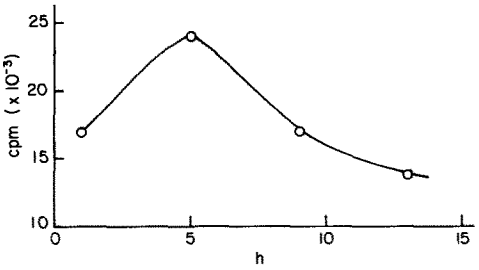

Figure 1. DNA Synthesis in subcultures started at G_1/S interphase cells. 3T3-B fibroblasts synchronized by double thymidine blocking were subcultured into 12-well tissue culture cluster (~1 $\times 10^5$ cells/ml DME containing 10% calf serum). Time zero started at 1 h after release from thymidine blocking. At the indicated times (○), they were incubated for 1-h periods with tritiated thymidine (10 Ci/mmol) and incorporation into DNA was measured with an LC 100C counter (liquid scintillation system; Beckman Instruments, Inc., Palo Alto, CA).

Results

Cell Synchronization

Before attempting to measure the effect of protein growth factors on the nuclear transport of exogenously incorporated fluorescent-labeled dextrans in a single living cell, it was essential to insure that the geometry of the cells remain approximately the same for accurate comparisons. In addition, the possibility of transport variation as a function of cellular position in the cell cycle necessitated an appropriate means to synchronize the cells. In an attempt to reduce both of these sources of cell-to-cell variation, we chose to synchronize our cells using double thymidine blocking (1). As calculated from tritiated thymidine incorporation measurements, BALB/c 3T3 fibroblasts had an S phase of ~10 h, G_1 ~6 h, and G_2/M ~5 h. This was consistent with observed doubling times of 20–21 h for this cell line. Unless otherwise stated, all measurements were performed on flat adherent (spread) cells within 4–6 h after releasing. Both 3T3-B and 3T3-KMuSV (data not shown) cells were restricted to the G_1/S interphase in the cell cycle as shown in Fig. 1.

Fluorescent Dextran Incorporation and Quantitation

Using the scrape-loading technique originally demonstrated by McNeil et al. (18) and modified by us (26), we attempted to incorporate fluorescent dextrans of 20,000 and 70,000 mol wt into the cell cytoplasm to serve as neutral transport probes. Since dextrans are not constitutive elements of normal cells and should not have potential nuclear localization and binding sequences (15), it was felt that these molecules would be capable of strictly reflecting changes in the transport rate initiated by protein growth factors. The results of this incorporation strategy are presented in Fig. 2. Using the ACAS 470 Interactive Laser Cytometer (Meridian Instruments, Inc.), a pseudo-color map was generated showing distribution of fluorescence intensity. As can be observed in Fig. 2 *a*, for the 20K dextran, the highest fluorescence intensities are found in the cell nuclei (*arrow*), while the cells containing 70K dextran show cytoplasmic labeling but minimal nuclear labeling (Fig. 2 *b*, *arrow*). When the data is replotted with fluorescence intensity represented on the *z*-axis, three-dimensional plots of the cellular distribution of fluorescence intensities are created (Fig. 2, *c* and *d*). The peaks in Fig. 2 *c* (red tops) clearly show the labeling of the nuclear vol-

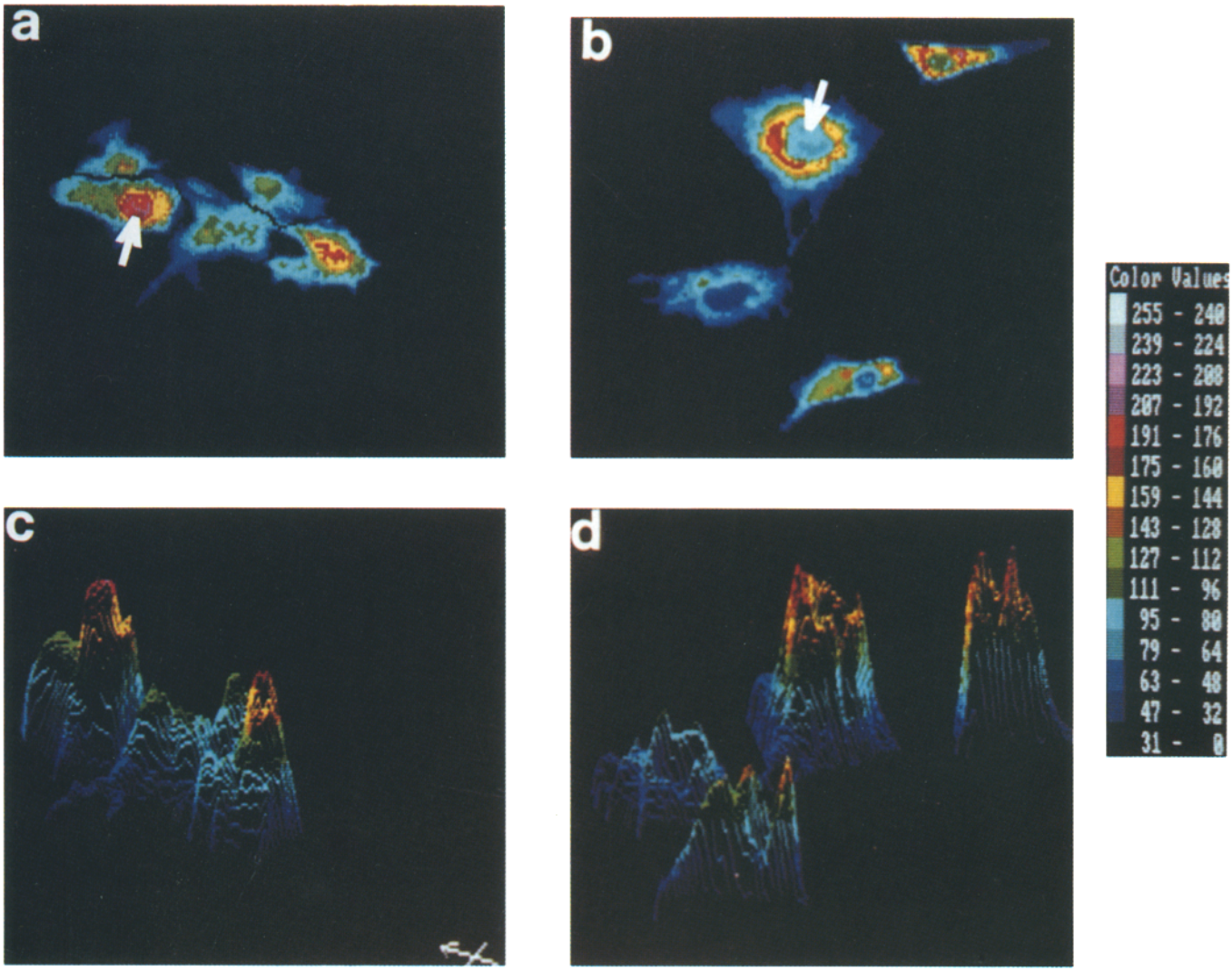

Figure 2. Pseudocolor digitized computer image of fluorescence intensity distribution of 20K and 70K fluorescein-derivatized dextrans in BALB/c 3T3 cells. 20K dextrans scrape-loaded into cells (Materials and Methods) reveal nuclear localization (*a*), while 70K dextrans are excluded from the nucleus (*b*). The images observed in *a* and *b* are now presented as a three-dimensional plot with intensity as the *z*-axis; *c* and *d* are three-dimensional representations of *a* and *b*, respectively. The arrows indicate the internally labeled nucleus. Color values are shown with their numerical equivalency.

ume, while the "crater" appearance of the 70K-incorporated cells (Fig. 2 *d*) are representative of little intranuclear accumulation. An important element of this analysis for subsequent transport interpretation is the requirement that the incorporation of labeled dextrans into the cell cytoplasm is equivalent, i.e., 20K and 70K dextrans are taken up with equal efficiency, and that nuclear uptake occurs for a significant population of cells. Using the ACAS 470, cell populations (>100 cells) were analyzed with regard to nuclear labeling and equivalency of uptake for 20K and 70K dextrans. Fig. 3 presents a series of cell histograms in which cellular fluorescence intensity of individual cells is calculated through a pixel by pixel integration of the two-dimensionally imaged cell (as represented by the cell images in Fig. 2). This analysis is performed on a large number of cells and a histogram is prepared relating fluorescence intensity/cell to cell number in a manner directly analogous to cell DNA histograms prepared with a fluorescence based flow cytometer. Since the cells are flat and adhering to the growth surface, the excited fluorescence will be weighted towards the greatest cellular volume, which is the noncompressible spherical nucleus. In this manner, nuclear localization of dextrans in whole cells may be quantitated. As observed in Fig. 3 *a*, 104 cells were analyzed with 30% of the cells showing strong nuclear fluorescence (defined as intensity >8) for the 20K dextran and 6% for the 70K dextran (Fig. 3 *b*). Fig. 3, *c* and *d* demonstrate that the fluorescence/area of incorporated 20K and 70K dextrans presents a similar profile over a cell population, suggesting that the efficiency of uptake and total amount of fluorescent-labeled 20K and 70K incorporated into the cells is approximately the same.

Nuclear Fluorescence Photobleaching

Because 70K dextrans were shown to be excluded from fibroblast nuclei, all transport measurements were performed with incorporated 20K fluorescent-labeled dextrans. Cells were scanned with a laser beam (argon ion λ_{Ex} = 488 nm) and photobleached as described. An example of the data

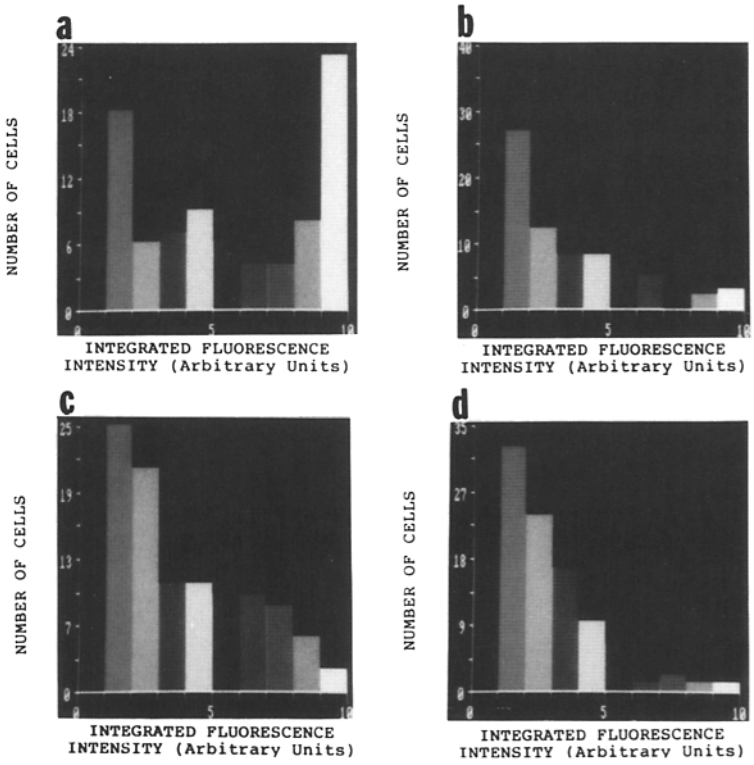

Figure 3. Histograms of 20K and 70K fluorescent dextran distribution in BALB/c 3T3 fibroblasts. *a* and *b* are histograms of fluorescent intensities (*x*-axis) for 104 cells scrape-loaded with 20K dextrans, and 111 cells loaded with 70K dextrans, respectively. *c* and *d* are the same as *a* and *b*, respectively, but represent the fluorescence/unit area (pixel).

obtained is presented in Fig. 4. An initial series of scans demonstrates a prebleach fluorescence level. A photobleach was initiated using a beam whose width is approximately that of the labeled nucleus (~6 μm in diameter). The photobleaching depletes the fluorescence in the nucleus, resulting in the decrease in intensity observed in scan *a* which is generated immediately after the bleaching event. Recovery of fluorescence as a result of nucleocytoplasmic transport is represented by the return to prebleach fluorescence levels. This is indicated by curves *b*, *c*, and *d* in Fig. 4 and additional unlabeled recovery curves. These recovery curves are analyzed and transformed into recovery rates as described. This technique was used to measure the nucleocytoplasmic transport rate of 20K dextrans in BALB/c 3T3 and 3T3-1 fibroblasts as a function of EGF concentration. The results presented in Fig. 5 demonstrate a saturable dose response for

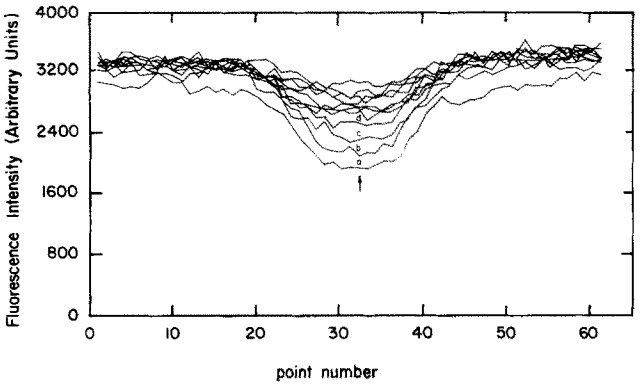

Figure 4. In vivo fluorescence photobleach of a BALB/c 3T3 nucleus loaded with 20K fluorescent-labeled dextrans. The ordinate is an arbitrary scale of fluorescence intensity, while the abscissa represents the position of the beam along a programmed scan. Each scan is a pass of the excitation laser beam across the nucleus. The interval between two scans, i.e., scan time with delay, is 5–10 s. A bleaching pulse results in the depletion of nuclear fluorescence represented by *a*; subsequent scans observed at nonbleaching excitation levels demonstrate fluorescence recovery (*b*, *c*, and *d*). The arrow represents the center of the bleaching pulse. The recovery of fluorescence is observed in a monitoring period of 2.5–5 min and is proportional to the dextran flux rate (12, 16). Beam diameter is ~6 μm.

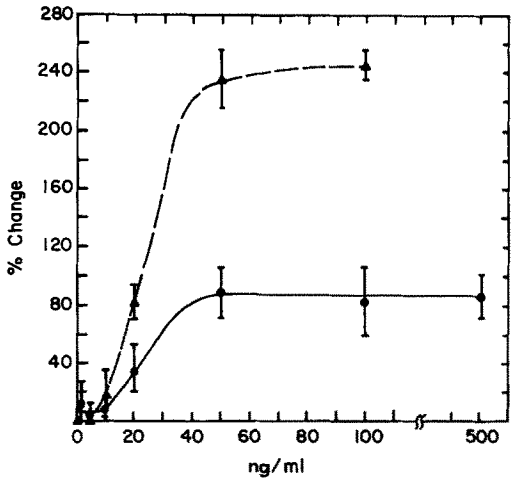

Figure 5. Dose dependence of EGF on dextran flux in BALB/c3T3 fibroblasts. The change in the rate of dextran transport of 20K fluorescent dextrans from control cells (●). A similar measurement performed on isolated rat liver nuclei using fluorescent-labeled 64K dextrans as the probe molecule (▲).

Table I. Effect of Cell Shape on Nucleocytoplasmic Transport of 20K Dextrans in 3T3 Fibroblasts

Conditions‡	Transport Rate*	
	3T3-1	BALB/c 3T3-KMuSV§
	10^{-3} s^{-1}	10^{-3} s^{-1}
Spread‖	6.4 ± 1.6¶ (8)**	18.9 ± 4.3 (7)
Spherical‡‡	6.4 ± 1.3 (8)	12.0 ± 2.0 (9)
Spherical + 40 ng/ml EGF	6.2 ± 0.5 (8)	–
Spherical + 500 ng/ml EGF	8.6 ± 2.5 (10)	–

* Transport rate constant of 20K dextran molecules.
‡ Cells in G_1/S interphase were obtained as described in Materials and Methods.
§ KMuSV-transformed BALB/3T3 fibroblasts.
‖ Cells were grown in DME (no calf serum supplement) and spread on 35-mm tissue culture dishes coated with fibronectin (50 μg/dish).
¶ Mean ± SD.
** Number of experiments.
‡‡ Cells were suspended in DME (no calf serum) immediately after scrape-loading with 20K dextrans.

EGF on nucleocytoplasmic transport in 3T3-B fibroblasts. All transport measurements were performed 1–2 h after adding EGF to the culture medium and incubation at 37°C. The nuclear transport rates dropped ~40% after 6-h incubation. This may be related to the reported decrease in EGF binding after ~6 h at 37°C (2). For comparison, the same series of measurements are presented for isolated rat liver nuclei (Fig. 5). Although the transport rate enhancement was ~2.5–3-fold higher in isolated rat liver nuclei (using 64K-mol-wt dextrans, the diameter of the nuclear pore complex in isolated rat liver nuclei appears to be larger [12, 16]), the concentration for half-maximal enhancement was approximately the same for both, 20–25 ng/ml (~3–4 nM).

Effect of Insulin and EGF on 3T3 and Kirsten Murine Sarcoma Virus-transformed 3T3 Fibroblasts

The previous results suggested that a dose dependent modification of nuclear macromolecular transport could be observed for EGF. More importantly, these effects occurred within the concentration range of EGF used for receptor–EGF-binding studies (from nuclear accumulation studies, on 3T3-1, half-maximal binding to nuclei occurred at ~1–3 nM EGF; M. Schindler and L.-W. Jiang, manuscript in preparation). The next question pursued was whether EGF and insulin could also affect this transport in transformed cells. For this study, KMuSV-transformed BALB/c 3T3 fibroblasts were used. The results of these experiments are presented in Tables I and II. Table I establishes that transformation results in an enhancement of macromolecular transport by ~200% over control when cells are attached and spread on the growth surface. Of particular interest is the apparent shape dependency for transport noted for the transformed cells. Spherical 3T3-KMuSV cells (nonadhering) have decreased transport rates, while 3T3-1 rates remain unchanged. Significantly though, untransformed cells in the

Table II. Effect of Protein Growth Factors and Transformation on Nucleocytoplasmic Transport

Conditions‡	Dextran transport rate*	
	3T3-1	BALB/c 3T3-KMuSV§
	10^{-3} s^{-1}	10^{-3} s^{-1}
Control (spread)‖	6.4 ± 1.6¶ (8)**	18.9 ± 4.3 (7)
+ 10 ng/ml EGF‡‡	11.3 ± 1.6 (6)	–
+ 20 ng/ml EGF	14.3 ± 2.6 (7)	–
+ 50 ng/ml EGF	19.8 ± 3.7 (8)	–
+ 500 ng/ml EGF	19.7 ± 3.0 (19)	19.4 ± 2.6 (7)
+ Boiled 500 ng/ml EGF	6.7 ± 1.2 (8)	19.0 ± 2.0 (5)
+ 40 ng/ml insulin	14.6 ± 2.2 (5)	–
+ 500 ng/ml insulin	18.9 ± 2.7 (13)	21.0 ± 4.7 (12)
+ Boiled 500 ng/ml insulin	6.9 ± 1.6 (8)	20.2 ± 3.4 (5)
+ 0.1 μg/ml insulin A chain	7.0 ± 1.1 (9)	–
+ 5 μg/ml glucagon	7.2 ± 2.6 (9)	21.0 ± 4.0 (6)
+ 10% calf serum§§	10.7 ± 2.7 (12)	22.0 ± 3.5 (18)
– Fibronectin‖‖	6.8 ± 1.3 (8)	–

* Transport rate constant of 20K dextran molecules.
‡ Cells in G_1/S interphase were obtained as described in Materials and Methods.
§ KMuSV-transformed BALB/3T3 fibroblasts.
‖ Cells were grown in DME (no calf serum) and spread on 35-mm tissue culture dishes coated with 50 μg/dish fibronectin, no EGF or insulin addition.
¶ Mean ± SD.
** Number of experiments.
‡‡ Transport measurements were performed after adding EGF to culture medium and incubating at 37°C for 1–2 h.
§§ Cells were growing in DME containing 10% calf serum.
‖‖ Cells were growing in DME and spread on tissue culture dishes without fibronectin coating.

spherical state have lost their ability to respond to EGF stimulation of nuclear transport even at extremely high EGF concentration (500 ng/ml). Table II shows that insulin and EGF are capable of significantly enhancing transport in untransformed cells, while boiled insulin and boiled EGF have no such effect. Glucagon and insulin A chain, at high concentrations, also did not affect transport. The effect of fibronectin removal was also examined and found to be without consequence as long as the cells remained attached and spread. The addition of calf serum to spread cells, as might be expected considering its content of growth factors, proved to be stimulatory. Of particular note is the observation that insulin and EGF had no effect on the already enhanced transport rate observed for the KMuSV-transformed cells (Table II).

Effect of EGF on Nuclear Transport in 3T3-NR6 Fibroblasts

Pruss and Herschman (20) isolated an EGF-nonresponsive cell line from murine Swiss albino 3T3 fibroblasts. Analysis of this EGF-nonresponsive variant demonstrated the absence of EGF receptor-related molecules and mRNA for the EGF receptor (29). When 20K dextran nuclear transport was examined in these cells under adherent conditions as described in Materials and Methods and Tables I and II, the addition of 200 ng/ml of EGF did not induce any transport rate enhancement. The rate in 3T3-NR6 without EGF was $7.1 \pm 1.0 \times 10^{-3}s^{-1}$, while in the presence of EGF (200 ng/ml) the transport rate constant is $7.4 \pm 1.5 \times 10^{-3}s^{-1}$. These values are nearly identical to control 3T3-1 fibroblasts and provide evidence that the EGF stimulation is receptor mediated.

Discussion

"Peptide hormone interactions with nuclei are a class of annoying data produced by good investigators, that is a class of pests that won't go away and that must be noticed" (quotation from an anonymous *Journal of Cell Biology* reviewer). Previous results provided evidence that EGF and insulin significantly stimulated macromolecular transport across the nuclear pore complex in isolated rat liver nuclei. This transport enhancement was demonstrated to be dose dependent and found to occur in the concentration range of reported physiological responses to these protein growth factors, e.g., nanomolar range (29). In consideration of these in vitro results, it may be appropriate to suggest that the protein growth factor stimulation of 3T3 fibroblast nuclear transport is dependent upon the delivery of protein growth factor or the growth factor/receptor complex to the nuclear surface. This may not only be inferred from the in vitro nuclear activation results (21, 25, 30), but is consistent with morphological evidence localizing monomeric ferritin-labeled insulin after 1–2 h to the perimeter of condensed chromatin, in particular near nuclear pores in 3T3-L1 adipocytes (32). Other morphological investigations also suggest a perinuclear localization of endocytosed protein growth factor receptors (8, 19). A chromatin localization for EGF, nerve growth factor, and platelet-derived growth factor was also reported by Rakowicz-Szulczynska et al. (22) after cellular subfractionation. The similarity between the dose dependency for protein growth factor binding to plasma membrane receptors (2–4, 24) and the dose response for activation of nuclear macromolecular transport suggest that either the nuclear protein growth factor/receptor complex is translocated from the cell surface and maintained in dynamic equilibrium with surface receptors, or indigenous nuclear receptors exist at the inner nuclear membrane/matrix interface that have similar protein growth factor-binding properties to plasma membrane receptors. These putative nuclear protein growth factor receptors would be activated by the delivery of protein growth factor from the plasma membrane.

Shape Modulation of Nuclear Transport

Our observation that shape plays a role in the protein growth factor stimulation of nuclear activity (spherical cells showed no nuclear transport enhancement as a function of added EGF) may be viewed in the context of demonstrations by Folkman and Moscona (5) that cell shape is tightly coupled to DNA synthesis, growth, and cellular response to growth factors. Our results now refine these observations to suggest that nucleocytoplasmic transport may be an important control point for shape modulation of cellular activity. The observation that spread and spherical cells have similar nuclear transport rates in the absence of calf serum or protein growth factors implies that under these limiting conditions, a relative basal transport rate is achieved that can then be enhanced only in the spread state after addition of EGF (Table I) or 10% calf serum (Table II). A model may be envisioned in which the mediation of a protein growth factor signal requires the organization of transport routes for the protein growth factor/receptor complex between the plasma membrane and nuclear surface. These transport tracks exist fully organized in nontransformed spread adhering cells, but not in spherical cells.

Transformation Enhances Nuclear Transport

Transformation of 3T3 fibroblasts with KMuSV results in maximal nuclear transport rates. Addition of high amounts of EGF, insulin (500 ng/ml), or 10% calf serum have no further enhancing effect. These observations fit well with the concept that transformed cells are self-stimulating (autocrine) and no longer require external protein growth factors (33). Since shape modification in this instance alters nuclear transport activity slightly, it may be possible that although autocrine self-stimulation appears to bypass normal cellular shape response mechanisms, some cellular structures for signal transmission are still moderately responsive to shape alteration.

Protein Growth Factor Nuclear-signaling Pathway: How Many Nuclear Receptors Are Enough?

In this discussion, we have presented evidence that protein growth factor-induced nuclear stimulation reflects growth factor/receptor occupancy at the nuclear surface. Under most assay conditions, the amount of protein growth factor found in the nucleus may be <2% of the total growth factor binding to the cell (13, 24, 32; L.-W. Jiang and M. Schindler, unpublished results). Is a 2% protein growth factor delivery efficiency sufficient to modify nuclear activity? In this context, it should be noted that although >90% of internalized growth factor/receptors may be targeted to the lysosomes (14, 19) or transported to other intracellular targets, the number of functional activated receptors necessary to induce trans-

port changes in the nucleus may be small. Protein growth factor receptors, in the presence of ligand, have been demonstrated to function as tyrosine kinases with very low activity in the absence of the ligand (10). Upon growth factor binding, endogenous enzymatic activity is greatly stimulated in the manner of allosteric activation, resulting in an activated receptor enzyme or "receptorzyme" (27). The activation of enzymatic activity would suggest that only a small number of receptorzymes need be captured by the nucleus to either activate indigenous nuclear receptorzymes or directly affect a number of mechanisms that result in the alteration of nuclear transport properties. Evidence now exists which shows that changes in polyphosphoinositide metabolism and phosphorylation/dephosphorylation of nuclear envelope components can vary the structural and transport properties of the nuclear pore complex (12, 21). Both biochemical signaling events have been associated with protein growth factor stimulation and oncogene-mediated transformation (9, 23). Previous reports in the literature provide good evidence that transformation of cells permit growth factor autonomous growth which is suggested to reflect an alteration of protein growth factor receptor or postreceptor-signaling pathway (33). Our results now extend these observations to show that transformation also results in the augmentation of the protein growth factor receptor response pathway to make nuclear transport activation independent of exogenous protein growth factor concentration. The results reported extend the analysis of cellular signaling from the cell surface to the nuclear envelope. Specific transport steps, particularly in relation to organized transcellular cytoskeletal pathways between the two signaling sites, and the nature of the nuclear envelope associated activator are presently under investigation.

We are indebted to Meridian Instruments, Inc. (Okemos, MI) for the use of an ACAS 470 Interactive Laser Cytometer.

This work was supported by National Institutes of Health grant GM 30158.

Received for publication 27 May 1987, and in revised form 9 October 1987.

References

1. Adams, R. L. P. 1980. Cell Synchronization. *In* Cell Culture for Biochemists. T. S. Work and R. H. Burdon, editors. Elsevier/North Holland, Amsterdam/New York/Oxford. 163–181.
2. Carpenter, G., and S. Cohen. 1976. ^{125}I-labeled human epidermal growth factor: binding, internalization, and degradation in human fibroblasts. *J. Cell Biol.* 71:159–171.
3. Carpenter, G., L. King, and S. Cohen. 1978. Epidermal growth factor stimulates phosphorylation in membrane preparations in vitro. *Nature (Lond.).* 276:409–410.
4. Cohen, S., R. A. Fava, and S. T. Sawyer. 1982. Purification and characterization of epidermal growth factor receptor/protein kinase from normal mouse liver. *Proc. Natl. Acad. Sci. USA.* 79:6237–7241.
5. Folkman, J., and A. Moscona. 1978. Role of cell shape in growth control. *Nature (Lond.).* 273:345–349.
6. Goidl, J. A. 1979. Insulin binding to isolated liver nuclei from obese and lean mice. *Biochemistry.* 18:3674–3679.
7. Goldfine, I. D., and G. J. Smith. 1976. Binding of insulin to isolated nuclei. *Proc. Natl. Acad. Sci. USA.* 73:1427–1431.
8. Haigler, H., J. F. Ash, S. J. Singer, and S. Cohen. 1978. Visualization of fluorescence of the binding and internalization of epidermal growth factor in human carcinoma cells A-431. *Proc. Natl. Acad. Sci. USA.* 75:3317–3321.
9. Hokin, L. E. 1985. Receptors and phosphoinositide-generated second messengers. *Annu. Rev. Biochem.* 54:205–235.
10. Hunter, T., and J. A. Cooper. 1985. Protein-tyrosine kinases. *Annu. Rev. Biochem.* 54:897–930.
11. James, R., and R. A. Bradshaw. 1984. Polypeptide growth factors. *Annu. Rev. Biochem.* 53:259–292.
12. Jiang, L.-W., and M. Schindler. 1986. Chemical factors that influence nucleocytoplasmic transport: a fluorescence photobleaching study. *J. Cell Biol.* 102:853–858.
13. Johnson, L. K., I. Vlodavsky, J. D. Baxter, and P. Gospodarowicz. 1980. Nuclear accumulation of epidermal growth factor in cultured rat pituitary cells. *Nature (Lond.).* 287:340–343.
14. Kahn, C. R., and K. Baird. 1978. The fate of insulin bound to adipocytes: evidence for compartmentalization and processing. *J. Biol. Chem.* 253: 4900–4906.
15. Kalderon, D., W. D. Richardson, A. F. Markham, and A. E. Smith. 1984. Sequence requirements for nuclear location of simian virus 40 large-T antigen. *Nature (Lond.).* 311:33–38.
16. Lang, I., M. Scholz, and R. Peters. 1986. Molecular mobility and nucleocytoplasmic flux in hepatoma cells. *J. Cell Biol.* 102:1183–1190.
17. Marchisio, P. C., L. Naldini, and P. Calissaro. 1980. Intracellular distribution of nerve growth factor in rat pheochromocytoma PC12 cells: evidence for a perinculear and intranuclear location. *Proc. Natl. Acad. Sci. USA.* 77:1656–1660.
18. McNeil, P. L., R. F. Murphy, F. Lanni, and D. L. Taylor. 1984. A method for incorporating macromolecules into adherent cells. *J. Cell Biol.* 98: 1556–1564.
19. Murthy, U., M. Basu, A. Sen-Majumbar, and M. Das. 1986. Perinuclear location and recycling of epidermal growth factor receptor kinase: immunofluorescent visualization using antibodies directed to kinase and extracellular domains. *J. Cell Biol.* 103:333–342.
20. Pruss, R. M., and H. R. Herschman. 1977. Variants of 3T3 cells lacking mitogenic response to epidermal growth factor. *Proc. Natl. Acad. Sci. USA.* 74:3918–3921.
21. Purrello, F., D. B. Burnham, and I. D. Goldfine. 1983. Insulin regulation of protein phosphorylation in isolated rat liver nuclear envelopes: potential relationship to mRNA metabolism. *Proc. Natl. Acad. Sci. USA.* 80: 1189–1193.
22. Rakowicz-Szulczynska, E. M.. U. Rodeck, M. Herlyn, and H. Koprowski. 1986. Chromatin binding of epidermal growth factor, nerve growth factor, and platelet-derived growth factor in cells bearing the appropriate surface receptors. *Proc. Natl. Acad. Sci. USA.* 83:3728–3732.
23. Rozengurt, E. 1986. Early signals in the mitogenic response. *Science (Wash. DC).* 234:161–166.
24. Savion, N., I. Vlodasky, and D. Gospodarowicz. 1981. Nuclear accumulation of epidermal growth factor in cultured bovine corneal endothelial and granulosa cells. *J. Biol. Chem.* 256:1149–1154.
25. Schindler, M., and L.-W. Jiang. 1987. Epidermal growth factor and insulin stimulate nuclear pore–mediated macromolecular transport in isolated rat liver nuclei. *J. Cell Biol.* 104:849–853.
26. Schindler, M., and L.-W. Jiang. 1987. Fluorescence redistribution after photobleaching as a tool for dissecting the control elements of nucleocytoplasmic transport. *Methods Enzymol.* 141:447–459.
27. Schindler, M., and L.-W. Jiang. 1987. Nuclear plasma membrane. Cytoplasmic communication. Linkages, controllers, pathways. *Comments Mol. Cell. Biophys.* 4:215–231.
28. Schindler, M., J. E. Trosko, and M. H. Wade. 1987. Fluorescence photobleaching assay of TPA inhibition of cell-cell communication. *Methods Enzymol.* 141:439–447.
29. Schneider, C. A., R. W. Lim, E. Terwilliger, and H. R. Herschman. 1986. Epidermal growth factor: nonresponsive 3T3 variants do not contain epidermal growth factor receptor-related antigens or mRNa. *Proc. Natl. Acad. Sci. USA.* 83:333–336.
30. Schumm, D. E., and T. E. Webb. 1981. Insulin-modulated transport of RNA from isolated liver nuclei. *Arch. Biochem. Biophys.* 210:275–279.
31. Shooter, E. M., B. A. Yankner, G. E. Landreth, and A. Sutter. 1981. Biosynthesis and mechanism of action of nerve growth factor. *Recent Progr. Horm. Res.* 37:417–447.
32. Smith, R. M., and L. Jarett. 1987. Ultrastructural evidence for the accumulation of insulin in nuclei of intact 3T3-L1 adipocytes by an insulin-receptor mediated process. *Proc. Natl. Acad. Sci. USA.* 84:459–463.
33. Sporn, M., and A. Roberts. 1985. Autocrine growth factors and cancer. *Nature (Lond.).* 313:745–747.
34. Vigneri, R., I. D. Goldfine, K. Y. Wong, G. J. Smith, and V. Pezzino. 1978. The nuclear envelope. The major site of insulin binding in rat liver nuclei. *J. Biol. Chem.* 253:2098–2103.
35. Wade, M. H., J. E. Trosko, and M. Schindler. 1986. A fluorescence photobleaching assay of gap junction-mediated communication between human cells. *Science (Wash. DC).* 232:525–528.
36. Yankner, B. A., and E. M. Shooter. 1979. Nerve growth factor in the nucleus: interaction with receptors on the nuclear membrane. *Proc. Natl. Acad. Sci. USA.* 76:1269–1273.
37. Yankner, B. A., and E. M. Shooter. 1982. The biology and mechanism of action of nerve growth factor. *Annu. Rev. Biochem.* 51:845–868.